

Journal Pre-proof

High denitrification potential but low nitrous oxide emission in a constructed wetland treating nitrate-polluted agricultural run-off

Ülo Mander, Julien Tournebize, Mikk Espenberg, Cedric Chaumont, Raili Torga, Josette Garnier, Mart Muhel, Martin Maddison, Jérémie D. Lebrun, Emmanuelle Uher, Kalle Remm, Jaan Pärn, Kaido Soosaar



PII: S0048-9697(21)01682-X

DOI: <https://doi.org/10.1016/j.scitotenv.2021.146614>

Reference: STOTEN 146614

To appear in: *Science of the Total Environment*

Received date: 13 January 2021

Revised date: 12 March 2021

Accepted date: 16 March 2021

Please cite this article as: Ü. Mander, J. Tournebize, M. Espenberg, et al., High denitrification potential but low nitrous oxide emission in a constructed wetland treating nitrate-polluted agricultural run-off, *Science of the Total Environment* (2021), <https://doi.org/10.1016/j.scitotenv.2021.146614>

This is a PDF file of an article that has undergone enhancements after acceptance, such as the addition of a cover page and metadata, and formatting for readability, but it is not yet the definitive version of record. This version will undergo additional copyediting, typesetting and review before it is published in its final form, but we are providing this version to give early visibility of the article. Please note that, during the production process, errors may be discovered which could affect the content, and all legal disclaimers that apply to the journal pertain.

High denitrification potential but low nitrous oxide emission in a constructed wetland treating nitrate-polluted agricultural run-off

Ülo Mander^{1,2*}, Julien Tournebize², Mikk Espenberg¹, Cedric Chaumont², Raili Torga¹, Josette Garnier³, Mart Muhel¹, Martin Maddison¹, Jérémie D. Lebrun², Emmanuelle Uher², Kalle Remm¹, Jaan Pärn¹, Kaido Soosaar¹

¹Department of Geography, Institute of Ecology and Earth Sciences, University of Tartu, Tartu, Estonia

²UR 1462 HYCAR, University Paris Saclay, French National Institute for Agriculture, Food, and Environment (INRAE), Antony, France

³UMR METIS, Sorbonne University CNRS EPHE, Paris, France

* Corresponding author: ulo.mander@ut.ee

Department of Geography, Institute of Ecology and Earth Sciences, University of Tartu, Vanemuise St. 46, 51014 Tartu, Estonia

Abstract

Constructed wetlands (CW) can efficiently remove nitrogen from polluted agricultural run-off, however, a potential caveat is nitrous oxide (N₂O), a harmful greenhouse gas and stratospheric ozone depleter. During five sampling campaigns, we measured N₂O fluxes from a 0.53 ha off-stream CW treating nitrate-rich water from the intensively fertilized watershed in Rampillon, France, using automated chambers with a quantum cascade laser system, and manual chambers. Sediment samples were analysed for potential N₂ flux using the He-O₂ incubation method.

Both inlet nitrate (NO₃⁻) concentrations and N₂O emission varied significantly between the seasons. In the Autumn and Winter inlet concentrations were about 11 mg NO₃⁻-N L⁻¹, and < 6.5 mg NO₃⁻-N L⁻¹ in the Spring and Summer. N₂O emission was highest in the Autumn (mean±standard error: 9.7±0.2 µg N m⁻² h⁻¹) and lowest in the Summer (wet period: 0.2±0.3 µg N m⁻² h⁻¹). The CW was a very weak source of N₂O emitting 0.32 kg N₂O-N ha⁻¹ yr⁻¹ and removing around 938 kg NO₃⁻-N ha⁻¹ yr⁻¹, the ratio of N₂O-N emitted to NO₃⁻-N removed was 0.033%. The automated and manual chambers gave similar results. From the potential N₂O formation in the sediment, only 9% was emitted to the atmosphere, the average N₂ : N₂O ratio was high: 89:1 for N₂-N_{potential} : N₂O-N_{potential} and 1353:1 for N₂-N_{potential} : N₂O-N_{emitted}. These results indicate complete denitrification. The focused principal component analysis showed strong positive correlation between the gaseous N₂O fluxes and the following environmental factors: NO₃⁻-N concentrations in inlet water, streamflow, and nitrate reduction rate. Water temperature, TOC and DOC in the water and hydraulic residence time showed negative correlations with N₂O emissions.

Shallow off-stream CWs such as Rampillon may have good nitrate removal capacity with low N₂O emissions.

Keywords: automated chambers; greenhouse gas; manual chambers; N₂; nitrate removal;

quantum cascade laser absorption spectrometer

1 Introduction

Nutrient export from anthropogenic activities in urban areas or agricultural fields harm water bodies through eutrophication and pollution of drinking water. Excess nutrients in freshwaters can be reduced efficiently by buffer zones and natural or constructed wetlands (CW; Verhoeven et al., 2006; Cheng et al., 2020). Nitrogen (N) is removed from the water via the following processes: (i) temporary direct plant uptake of inorganic N and sedimentation (Brix, 1997; Abe et al., 2014; Li et al., 2015); (ii) microbial N transformation into gaseous dinitrogen (N_2) via denitrification and anammox (Erler et al., 2008; Ligi et al., 2015; Wang et al., 2018; Ma et al., 2019), and (iii) nitrous oxide (N_2O) from denitrification (Erler et al., 2008; Jia et al., 2011; Batson et al., 2012), nitrification (Jia et al., 2011; Zhang et al., 2018) or DNRA (Jahangir et al., 2017; Wang et al., 2018). Although wetlands play a larger role in climate change mitigation through the carbon cycle, N removal may also contribute significantly through N_2O emissions, especially at higher N loading rates. N_2O is a greenhouse gas with a global warming potential about 153-310 times more powerful than carbon dioxide depending on the time horizon (IPCC, 2007), and it is 298 times larger in the 100 years timespan (IPCC, 2013). Moreover, N_2O has been predicted to be the dominant stratospheric ozone-depleting substance in the 21st century (Ravishankara et al., 2009).

Long-term monitoring in wetlands demonstrated that nitrate (NO_3^-) removal efficiency depends on climate conditions, input load, carbon availability, residence time, and vegetation cover (Pulou et al., 2011; Torneboize et al., 2017). However, few wetland studies have evaluated the environmental risks associated with NO_3^- removal and the balance between water quality improvement and N_2O emissions (Freeman et al., 1997). For instance, increased anthropogenic N loads potentially strengthen the risk for N_2O emissions in freshwater wetlands (Paludan & Blicher-Mathiesen, 1996; Wang et al., 2017; D'Acunha & Johnson, 2019) and salt marshes (Chmura et al., 2016). Most commonly, N_2O is a product of incomplete processes of denitrification or nitrification (Butterbach-Bahl et al., 2013). Complete heterotrophic denitrification ends up with production of dinitrogen (N_2 ; Wilcock & Sorrell, 2008; Butterbach-Bahl et al., 2013). Therefore, analysis of environmental conditions regulating both production and consumption of N_2O is crucial for evaluation of the net N_2O emission in ecosystems.

N_2O is highly soluble in water (Haynes, 2015). Therefore, in addition to the primary losses of the N_2O gas produced from nitrification and denitrification in the soil, the dissolution and eventual degassing of N_2O in leaching and drainage water from agricultural fields is also a

significant loss pathway (Dowdell et al., 1979; Roper et al 2013). N₂O fluxes from water bodies (degassing) in agricultural areas are considered as indirect N₂O emission. They are calculated as the proportion of the N leached from soils to the N applied as fertilizers. By default, this proportion is considered as 30% of the amount of applied N in fertilizers; Kasper et al., 2019). The partitioned emission factors for N₂O degassing from leached water, rivers and estuaries are 0.015, 0.0075, and 0.0025, respectively (IPCC, 2000, IPCC, 2002). However, recent publications propose degassing factors for the surface waters up to one order of magnitude lower (Sawamoto et al., 2005; Maavara et al., 2019). In a larger riverine system of complex land-use pattern, the indirect fluxes were estimated to account only for 3.7% of the total greenhouse gas emissions from the basin, while N₂O emissions accounted for 4.4% of all indirect fluxes (Marescaux et al., 2018). Beaulieu et al. (2011) found a high average emission rate (37 µg N₂O-N m⁻² h⁻¹) from US rivers, while Xiao et al. (2019) reported 1.5 times higher emissions from rivers and ditches of an agricultural watershed in Eastern China. Furthermore, emissions from shallow lakes vary remarkably, from -12 through 48 (Soja et al., 2014) to 969.2 µg N₂O-N m⁻² h⁻¹ (Liu et al., 2014) showing lower values in their littoral zone. Likewise, larger and cleaner lakes emit significantly less N₂O (Chen et al., 2011). In several studies, N₂O emissions were calculated from dissolved N₂O, as a water-atmosphere equilibrium in stream water (Garnier et al., 2009; Audet et al., 2017). Large concentrations of dissolved N₂O are shown in nitrate-contaminated groundwater (Vilain et al., 2012; Jurado et al., 2017) and eutrophic ponds (Cao et al., 2016) Although wetlands can be sinks for dissolved N₂O, they show low concentrations when compared to the inflowing groundwater or streamwater (Blicher-Mathiesen & Hoffmann, 1999; Hinshaw & Dahlgren, 2016; Wang et al., 2017), while low pH (< 0.6) in rivers may decrease dissolved N₂O concentration and increase degassing (Aude et al., 2020).

The proportion of denitrified NO₃⁻ that is converted to N₂O rather than N₂ – the N₂O yield – is usually applied to characterize the denitrification potential of aquatic ecosystems (Beaulieu et al., 2011). Likewise, the ratio of N₂ : N₂O in sediments is an important parameter of nitrogen cycle in water bodies, but only few ¹⁵N isotope studies considering the N₂ : N₂O ratio in wetland sediments are known from early 1990s (Lindau & DeLaune, 1991; Lindau et al., 1991).

For free water surface (FWS) CWs (Erler et al., 2008; Batson et al., 2012) as well as for wastewater stabilization ponds (Glaz et al., 2017) only limited information on N₂O investigations is available.

The main objectives of this study are: (1) to analyse N₂O emission dynamics in relation to

water quality and environmental factors and (2) to estimate the denitrification potential in an off-stream constructed wetland treating nitrate-polluted water from an intensively managed agricultural catchment. To meet the first objective, we applied a new methodology of semi-continuous measurement using a quantum cascade laser absorption spectroscopy (QCLAS) system, which allows high temporal frequency measurement of N_2O fluxes. For the second purpose, a novel He- O_2 incubation method of intact soil cores was implemented (Butterbach-Bahl et al., 2002). The manual chamber technique is a common method for the measurement of N_2O fluxes in CWs (Mander et al., 2014) and no previous attempt using automated chambers with N_2O analysers is documented. The latter is quite a common technique used in various other ecosystems for decades (Hargreaves et al., 1995; Yao et al., 2009). High-frequency laser systems are widely used to analyse N_2O fluxes in terrestrial ecosystems, mostly for eddy covariance studies (Eugster et al., 2007; Cowan et al., 2014; Huang et al., 2014; Merbold et al., 2014). However, these systems are still scarcely used in wetlands (Savage et al., 2014).

Considering the results from previous studies we hypothesize that: (1) the studied CW is a major source of gaseous N_2O emissions and (2) the denitrification potential of the sediments is high. To check these hypotheses, we aimed to (i) better understand N_2O emission dynamics at diurnal and seasonal time scales, (ii) analyse the dependence of N_2O flux on various environmental conditions, (iii) analyse the ratio of gaseous to dissolved N_2O fluxes, and (iv) determine the $N_2:N_2O$ ratio in the CW. Several continuous monitoring campaigns were carried out at key seasons in an experimental comprehensively studied CW within an agricultural watershed.

2 Material And Methods

2.1 Site description

2.1.1 Context of the study

The Champigny aquifer (limestone of the Eocene Epoch) is a major groundwater resource for Paris Area providing drinking water for more than 1.5 million inhabitants living in 1700 km². About 60% of the annual water reload of this karstic aquifer is directly infiltrated from surface water through natural sinkholes, increasing the vulnerability of the groundwater to diffuse source of pollution. We investigated a 355-ha watershed of Rampillon in the historic Brie region of Île-de-France (Paris Region) (Seine-et-Marne, (03°03'47" E, 48°32'19" N, 70 km south-east of Paris, France).

2.1.2 Rampillon constructed wetland

The Rampillon CW in the Brie plateau was implemented in 2010 to collect drainage and run-

off waters from an agricultural catchment and meet local environmental and health issues. The 5300 m² constructed wetland consists of ecologically engineered sub-basins separated by bunds to enhance water time retention and mitigation processes (Fig. 1). A first sedimentation sub-basin (deep inflow zone) is about 1 m deep and 300 m³ in volume. A middle zone of 5000 m² has a maximum 0.5 m depth with a volume max of 1200 m³. A 1000 m² with 0.8 m deep outflow sub-zone was implemented upstream from the outlet. In 2015, about 40% of the CW was covered by sedges (*Carex* spp.), common reed (*Phragmites australis*), broadleaf cattail (*Typha latifolia*), bulrushes (*Juncus* spp.) and various algae.

Five different campaigns were organized to cover the seasons of a full hydrological year. The beginning of the campaign in May 2014, with already high temperatures and low flow conditions, was classified as Spring. The end of May 2014 and October 2015 were classified respectively, as wet or dry Summer (Summer W or D, respectively), respectively. Summer D had no water flow and some parts of the CW sediments were dried up. Autumn was represented by November 2014, characterized by low temperature and intensive flow. Winter was represented by the March 2015 campaign, corresponding to low temperature, intensive water flow and the highest nitrate concentrations. The duration of a campaign was 3-6 days (Supplementary Table S1).

An automatic weather station (Campbell Scientific Inc., Logan, UT, USA) measured rainfall, solar radiation, air temperature and humidity at the wetland location.

2.2 Water quality measurements

Continuous water flow and quality monitoring system installed at the inlet and outlet of the CW measured flow turbidity, dissolved organic carbon (DOC), total organic carbon (TOC) and NO₃⁻ concentrations at hourly time step using a Doppler sensor (Sigma 950 Flow Meter; Hach Company, Loveland, CO, USA) and multiparameter spectrophotometer (spectro::lyser UV-vis; scan Messtechnik GmbH, Vienna, Austria). Hydraulic retention time (HRT) and nitrate retention ratio (RR-N) were calculated based on the flow dynamics and NO₃⁻ concentrations on inlet and outlet.

During the five campaigns, temperature, pH, electric conductivity (EC), dissolved oxygen concentration and its saturation were measured using portable devices (Multiparameter portable meter MultiLine® Multi 3630 IDS; and YSI ProODO Optical Dissolved Oxygen Meter; both by Xylem Analytics, Beverly, MA, USA). In each compartment of the CW, water samples for the analysis of daily nutrient concentration was sampled. Anions (SO₄²⁻, Cl⁻) and cations (NH₄⁺, K⁺, Na⁺, Ca²⁺, Mg²⁺) from all water samples (automatic and manual) were analysed at the lab of the UR HYCAR, French National Institute for Agriculture, Food,

and Environment (INRAE), Paris, using ion chromatography (DIONEX DX-120) with a pre-column Dionex IONPAC1 AG9-HC and a IONPAC1 AS9-HS column (Thermo Fisher Scientific Inc., Waltham, MA, USA). A 9-mM carbonate buffer solution was used as the mobile phase. Water temperature and water level were measured using a pressure transducer model Madofil by IRIS (IRIS Instruments, Orléans, France).

Water samples for dissolved N_2O analysis were collected at 5 to 8 different points of the wetland, about 2 to 5 times per campaigns between 10h and 12h of the daytime. Samples were stored in a 100 ml penicillin flask, poisoned with $HgCl_2$ (2%) and stoppered with a rubber septum excluding any headspace. In the laboratory of UMR METIS, Sorbonne University, Paris, dissolved N_2O was determined with a gas chromatograph Perichrom ST 2000 (Perichrom, Saulx-les-Chartreux, France) combined with an electron capture detector (GC-ECD) (Garnier et al., 2009; 2010).

2.3 N_2O measurements

2.3.1 Automated chamber measurements

A system of 12 automated floating chambers was connected via the multiplexer to a quantum cascade laser system (Aerodyne QCLAS N_2O - H_2O - CH_4 analyser; Aerodyne Research Inc, Billerica, MA, USA) for a continuous high frequency (1-2 Hz) monitoring of N_2O fluxes. This instrument uses tunable infrared laser differential absorption spectroscopy (TILDAS) enabling an on-line analysis of atmospheric trace gases with high sensitivity.

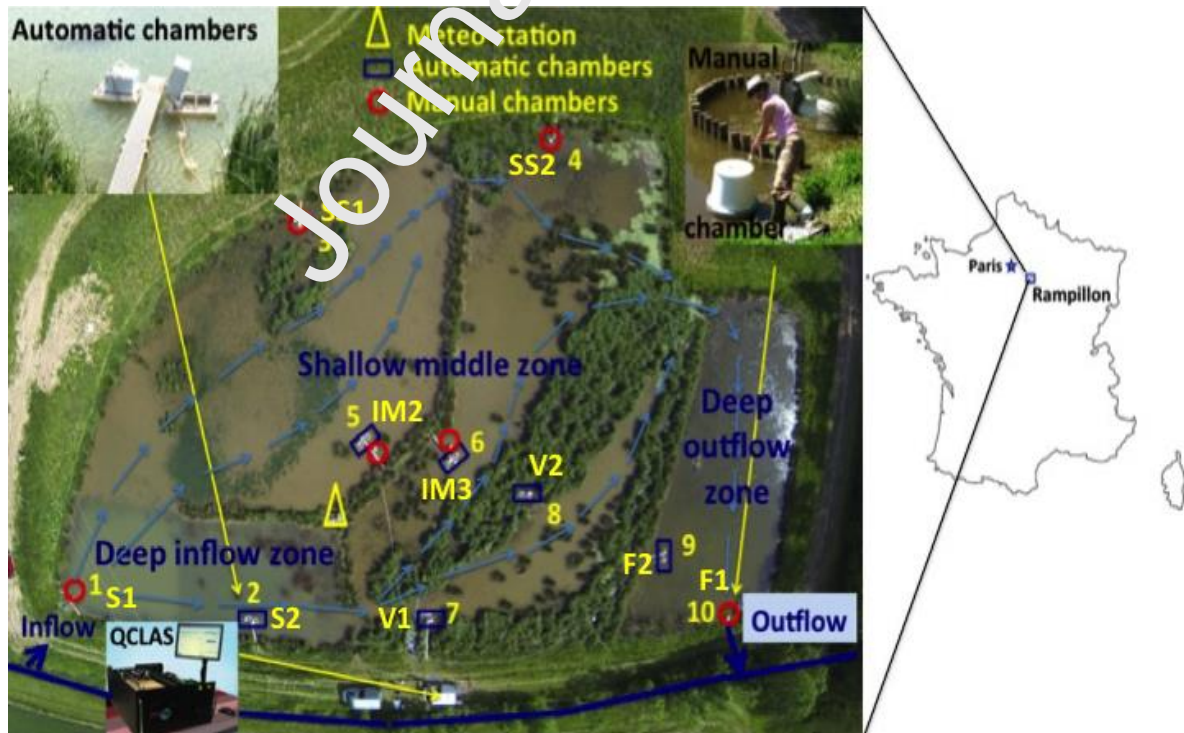


Figure 1. Location of Rampillon constructed wetland in France and set-up of chambers for

gas measurements (1-10) and sediment sampling points: deep water - S1, S2 (inflow) and F1, F2 (outflow); shallow and stagnant water – SS1, SS2, IM2, IM3, V2 and V2.

The laser frequency is 1271 cm^{-1} for N_2O , the system is thermoelectrically cooled (Thermocube) to 32°C . For a complete description of the QCLAS instrument, see Nelson et al. (2004). The QCLAS analyser was connected through pumps and PTFE pipes to the multiplexer linked to 12 chambers located in 6 pairs on the 30-35 m distance from the gas analyser installed in a van (Fig. 1). Each rectangular PVC chamber covered a 0.16 m^2 wetland surface, containing a volume of 0.032 m^3 . To avoid stratification of gas inside the chamber, air with a 1.8 L min^{-1} constant flow rate was circulated within a closed loop between the chamber and gas analyser unit during the measurements by a diaphragm pump. The air sample was taken from the top of the chamber headspace and pumped back by distributing it to each side of the chamber. For the measurements, the chambers were closed automatically for a duration of 6 minutes each. Flushing time of the whole system with ambient air between measurement periods was 1 minute. Thus, there were approximately 18 measurements per chamber per day. Each automated chamber was installed on a floating frame of extruded polystyrene foam. The frame was anchored to ensure stability in opening and closing and support the equilibrium of the water column.

The air temperature in the chamber was measured and used to convert the concentrations from ppm[v] to mg m^{-3} according to the ideal gas law before flux calculation (Collier et al., 2014). Gas fluxes were calculated for a selected time window (150 seconds), after discarding initial 90 seconds to exclude the initial stabilisation period, using the linear model which is based on the assumption of a linear relationship between concentrations inside the chamber headspace and time (Livingston & Hutchison, 1995).

2.3.2 Manual chamber measurements

Additional manual chamber measurements (Hutchinson & Livingston, 1993) were conducted to cover the whole wetland. Six of them were located in remote places where automated measurements were not possible to install. Four manual chambers were set up close to the automated chamber allowing a comparison between the short-term (1 hour) and continuous (several days) monitoring results (Fig. 1). Sampling was carried out twice a day (in the morning and in the afternoon). Gas samplers (opaque static PVC chambers of truncated-cone shape, height 50 cm, Ø 50 cm, volume 65 L, painted white to avoid heating during application; similar to those used in soil flux analyses; Mander et al., 2005) were installed on hollow-foam swimming-pool noodles and anchored for stability. Gas samples were taken

right after the closure of the chambers (0 moment) and after 20 min, 40 min and 60 min using pre-evacuated (0.3 mbar) 50-mL gas bottles (Hansen et al., 2013) to determine emission rates. Gas concentration in the samples was analysed using the Shimadzu GC-2014 gas chromatography system (Shimadzu Corporation, Kyoto, Japan) equipped with ECD detector modified by Loftfield et al (1997). The emission rate of trace gas was calculated based on the linear increase of gas concentrations in time, corrected with the area and volume of the chamber (Soosaar et al., 2011).

2.4. Sediment sampling and analysis

Sediment samples were taken before and after each campaign from two depths (0-5 cm and 10-15 cm) in 12 locations (Fig. 1) and analysed in dried sediment for pH_{KCl} and content of organic matter (OM), total carbon (TC) and total nitrogen (TN) using a varioMAX CNS elemental analyser, dissolved nitrogen (DN), TOC, DOC and dissolved inorganic carbon (DIC) using Vario TOC/TNb detector (Elementar Analyzentechnik GmbH, Langensfeld, Germany), and NO_3^- -N, NH_4^+ -N, total P, Ca and Mg according to standard methods (APHA-AWWA-WEF, 2005) at the laboratories of the University of Tartu and the Estonian University of Life Sciences. Ten intact sediment samples with metallic cylinders were taken from the 0-10 cm upper layer for further analysis of potential N_2 and N_2O fluxes in the gas chromatography lab of the Department of Geography, University of Tartu, Estonia. Helium atmosphere soil incubation technique was used to measure potential N_2 and N_2O fluxes from intact soil cores in laboratory (Butterbach-Bahl et al. 2002). The cylinders with the intact soil cores were placed into special gas-tight incubation vessels located in a climate chamber. Gases were removed by flushing with an artificial gas mixture (21.0% O_2 , 358 ppm CO_2 , 0.313 ppm N_2O , 1.67 ppm CH_4 , 5.97 ppm N_2 and rest He). The new atmosphere equilibrium by continuously flushing the vessel headspace with the artificial gas mixture at 20 mL per minute was established after 12-24 h. The flushing time depended on the soil moisture. The temperature was kept similar to the field conditions during incubation. The gas-chromatograph (Shimadzu GC-2014) equipped with a thermal conductivity detector was used to measure N_2 and N_2O concentration in the mixture of emitted gases accumulated in the headspace (0, 40, 80, and 120 minutes) of the cylinder after 2 h of closure. The gas concentration in the chambers increased in a near-linear way so that linear regression was applied for calculation of the fluxes. For all gas analyses only flux measurements leading to a R^2 of 0.81 or greater ($p < 0.01$) were used.

2.5. Statistical analysis of data

The data set was analysed by two complementary statistical methods: principal component

analysis (PCA) and focused PCA (FPCA). Differences in PCA between the sampling campaigns and subsites were evaluated using PERMANOVA with 9999 permutations. Pairwise comparisons were corrected with the Bonferroni method. Focused PCA allows determining the main factors explaining the variability of N₂O and N₂ emissions. Correlations between the dependent variable and the other variables are represented faithfully in FPCA, contrary to PCA. Randomesque missing values for both PCA and FPCA were imputed using the random forest technique. One-way ANOVA with the Tukey HSD post hoc test was applied to evaluate the significance of the differences between seasons in dissolved N₂O concentrations and ratios (N₂-N_{potential} : N₂O-N_{potential} and N₂-N_{potential} : N₂O-N_{emitted}). In addition, the t-test was used to evaluate the significance of the differences between ratios of N₂-N_{potential} : N₂O-N_{potential} and N₂-N_{potential} : N₂O-N_{emitted} according to each season. Exploratory data analyses were performed with the *missRANGE* (Mayer, 2019), *ade4* (Dray & Dufour, 2007), *vegan* (Oksanen et al., 2019) and *psy* packages (Falissard, 1999) of the R software.

3 Results

3.1 Water regime and quality at inlet and outlet

During the campaigns, hydrological regimes were relatively stable due to low rainfall and low maximum flows in response to high rainfall events: from no flow during the summer campaign to 5.9 and 14.8 L s⁻¹ for the Autumn and Winter campaigns respectively (Fig. 2, Table 1). Discharge during the campaigns was representative for 82% of a full hydrological year while the discharge above 15 L s⁻¹ represented the rest of time. Water depth was above full storage in CW during the Autumn, Winter and Spring but low during the Summer W and Summer D campaigns. Inlet flow was zero during the Summer W and D events, low (2.5 L s⁻¹), and Spring, and high during Autumn and Winter (29.4 and 26.8 L s⁻¹, respectively).

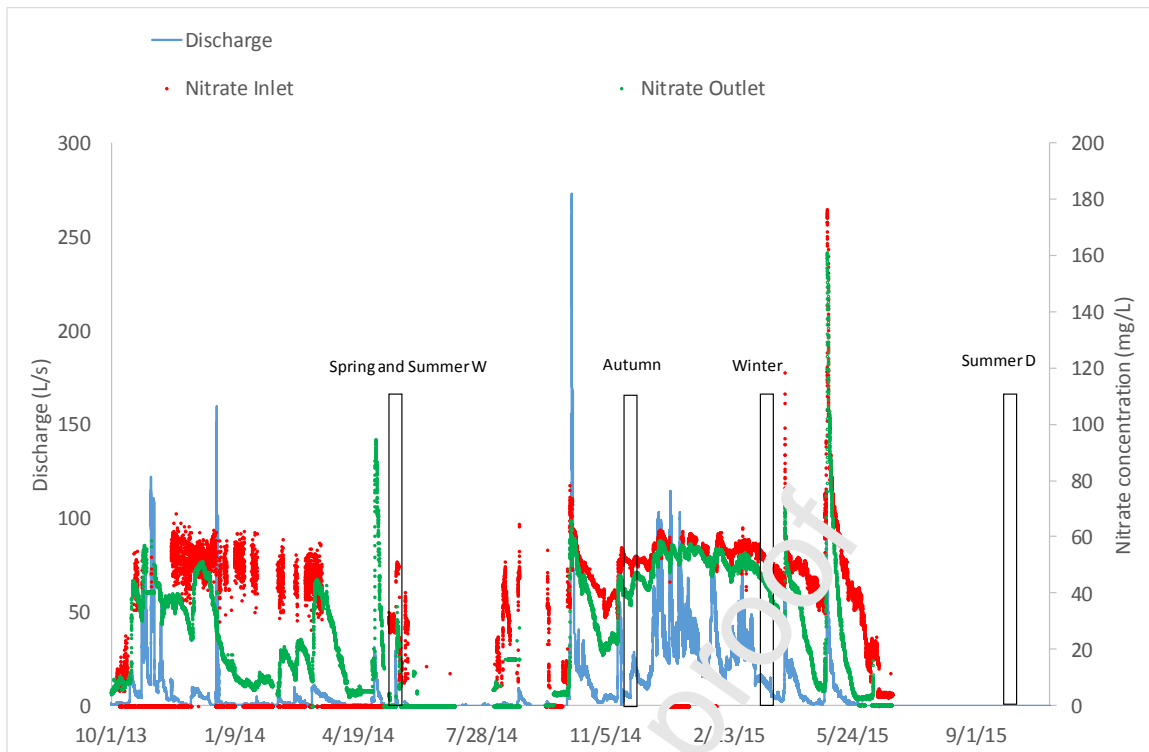


Figure 2. Discharge and nitrate concentrations at the inlet and outlet of the Rampillon CW during the period 2013-2015. Black rectangles indicate five campaigns: Spring and Summer W in May 2014, Autumn in November 2014, Winter in March 2015, and Summer D in October 2015.

The corresponding theoretical hydraulic residence time ranged from short (2 or 4 days) during Autumn and Winter to long (216 days) during Spring and could not be calculated for the no-flow period of Summer W and D.

The dynamics of nitrate concentrations during the campaigns was representative for 75% of the full drainage season. In general, the CW reduced NO_3^- concentrations from inlet water (Fig. 2). Nitrate concentrations were higher during Autumn and Winter (about $11 \text{ mg NO}_3^- \text{-N L}^{-1}$) and lower during Spring and Summer ($< 6.5 \text{ mg NO}_3^- \text{-N L}^{-1}$). The average nitrate removal rate in Autumn, Winter and Spring varied from 0.08 to $0.64 \text{ mg NO}_3^- \text{-N m}^{-2} \text{ d}^{-1}$. The negative removal value ($-0.13 \text{ mg NO}_3^- \text{-N m}^{-2} \text{ d}^{-1}$) in Summer W was explained by the water management strategy: the inlet was closed, but the outlet gate kept open (Table S1). NO_3^- concentrations in the water at different points within the CW were similar to the outlet measurements for all campaigns. The other water quality variables showed limited changes, e.g. pH only varied between 7.4 and 7.6, and no difference was detected for NH_4 neither at inlet/outlet nor in the ponding water. Dissolved oxygen exhibited the highest diurnal and seasonal variation from 79% to oversaturation 143% in Winter, including a high standard

variation coefficient (36% during Spring and Summer W). DOC and TOC measurements showed a stable value throughout the campaigns, nevertheless there was a big difference between the inlet and outlet values: 22.2 and 5.0 DOC mg L⁻¹ and 46.8 and 43.6 TOC mg L⁻¹ respectively.

3.2 Sediment characteristics

Based on the texture (clayed silt soil, with 28%, 62% and 10% clay, silt and sand respectively), the sediment of this CW is similar to the typical Luvisols of the Paris Region. Physical-chemical characteristics of sediments showed some spatial and seasonal variability. The following ones demonstrated relatively high stability: (i) pH (mean value varied from 7.35 to 7.62), (ii) TN content (0.13 to 0.16%), (iii) TC/TN ratio (14.1 to 19.0), and (iv) OM content (2.3 to 3.1%). Also, the sediment is characterized by a relatively high and stable concentration of Ca and Mg (average values varied 2642-3830 and 67-86 mg kg⁻¹, respectively).

The contents of NH₄⁺, NO₃⁻ and COD, as well as the TC/TN ratio showed a relatively large range of temporal-seasonal variations (see Table S1). NH₄⁺ contents were three-fold lower in the shallow part to compare with the deeper zones close to inlet and outlet, and likewise, the seasonal variability was relatively high (14-39 mg kg⁻¹). The NH₄⁺ contents were much higher than NO₃⁻ content (0.26 mg kg⁻¹), likely due to denitrification in the anoxic area. The seasonal variability of sediment NO₃⁻ contents ranged between low content in Autumn and Winter (0.03 mg kg⁻¹), intermediate in Spring (0.17 mg kg⁻¹) and high in Summer D (0.88 mg kg⁻¹). DOC content varied from 59 mg kg⁻¹ and 133 mg kg⁻¹ in Summer D and Spring, respectively, linked to the development of vegetation (e.g., C source for the root zone). Nevertheless, the TC/TN ratio of the sediment was about 10, considered as not limiting for the denitrifying processes although carbon biodegradability was not assessed.

3.3 Gaseous N₂O emissions

3.3.1 Seasonal and diurnal patterns of N₂O emissions

Annual average N₂O emission from the Rampillon CW calculated either from automated or manual chambers was relatively low: 3.9 or 3.6 µg N₂O-N m⁻² h⁻¹, respectively (Fig. 3).

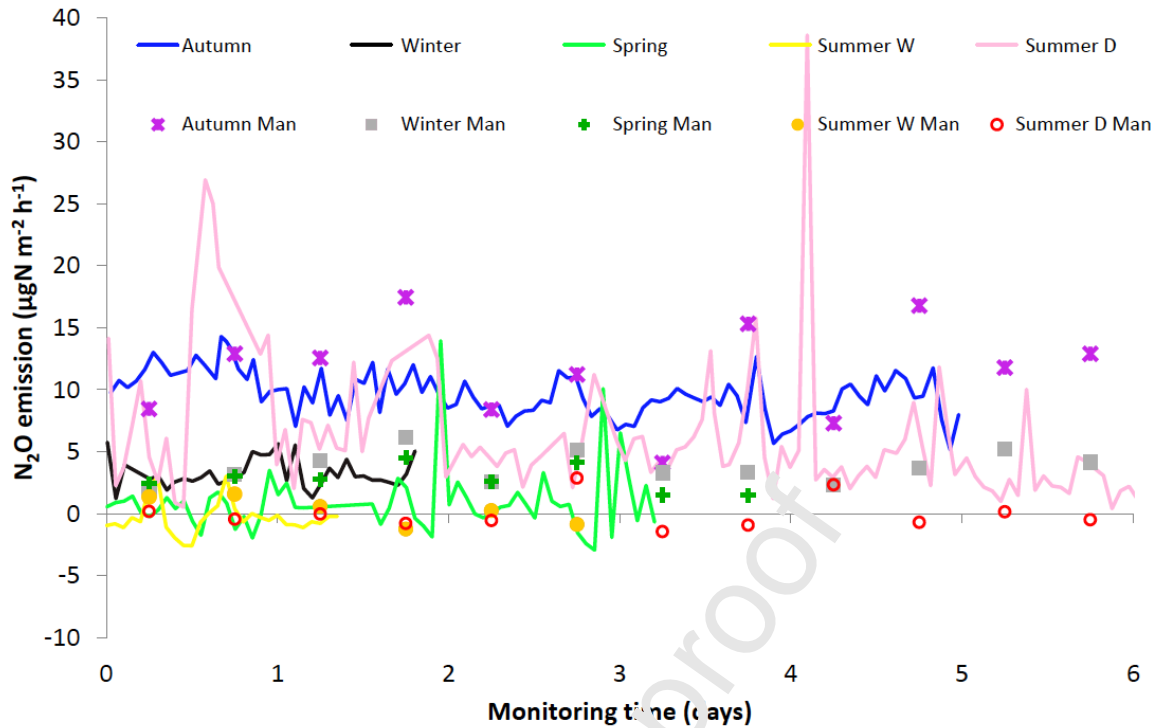


Figure 3. The daily evolution of N₂O emissions in Rampillon constructed wetland during the five seasonal campaigns using automated (line) and manual (point, Man in legend) chamber techniques.

The range of individual values was -8.5 to $138 \mu\text{g N}_2\text{O-N m}^{-2} \text{h}^{-1}$. The seasonal variation of N₂O emissions was moderate (Table 1). Autumn's and Winter's emissions showed relatively stable values similar between the automated and manual chambers: Autumn: 9.2 vs 11.4 and Winter: 2.6 vs $3.8 \mu\text{g N}_2\text{O-N m}^{-2} \text{h}^{-1}$ respectively. Spring values between the automated and manual chambers were also in the same range (mean values 0.9 vs $1.6 \mu\text{g N}_2\text{O-N m}^{-2} \text{h}^{-1}$, respectively). Summer W emissions were very low (0.1 and $1.8 \mu\text{g N}_2\text{O-N m}^{-2} \text{h}^{-1}$ in automated and manual chambers, respectively) showing negative values (-2.59 and $-1.26 \mu\text{g N}_2\text{O-N m}^{-2} \text{h}^{-1}$) at the end of the second day for both techniques. As expected from the differences in chamber positioning (see method section), during the Summer D period, average N₂O fluxes measured with automated chambers were three magnitudes higher than those determined by manual chambers: 5.4 and $-0.01 \mu\text{g N}_2\text{O-N m}^{-2} \text{h}^{-1}$, correspondingly. Summer D data from automated chambers showed the largest variability: individual values varied from -0.9 to $85 \mu\text{g N}_2\text{O-N m}^{-2} \text{h}^{-1}$.

The graph of cumulative fluxes of gaseous N₂O demonstrates a rather linear increase during all the seasons and over all the chambers (Fig. 4). Although the diurnal variability of N₂O fluxes was large (40%), cumulative emissions measured with high-frequency technique or

calculated based on two-day data with the manual method, were linear for the six consecutive days of the experiment. The comparison between manual and automated techniques shows congruent values in four out of the five campaigns (Fig. 4; Supplementary Figures S1 and S2). Without the values from the exceptional Summer D period the correlation between the data gathered using the two techniques was significant ($R^2 = 0.53$; $p < 0.01$; Fig. S2).

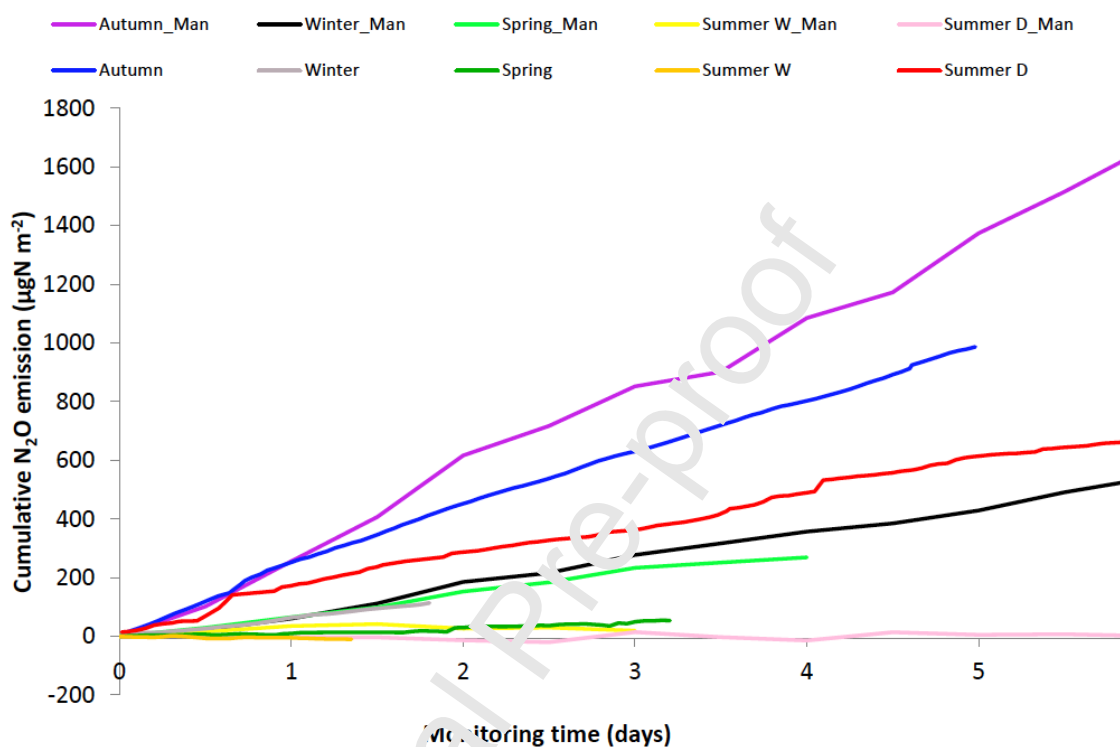


Figure 4. Cumulative N₂O emissions measured by the automated and manual chamber techniques calculated across the five campaigns. Man – manual chambers.

The high-frequency measurements enabled us to evaluate the diurnal variability of N₂O emissions. All campaigns exhibited a high variability of emission values within a day: from 38% in Autumn to 176% in Summer W (Fig. S1). The maximum peak emissions often occurred at the maximum solar radiation around 14h for Autumn and Winter, around 16h for Spring and Summer W and largely up to 21h for Summer D (all times are in GMT+2).

3.4 Dissolved N₂O

Dissolved N₂O exhibited remarkable variations (Fig. S3). During Winter no water samples contained dissolved N₂O. Autumn and Spring showed similar values around 12.7 µg N₂O-N L⁻¹. During the warm Summer W, dissolved N₂O level was intermediate (8.2 µg N₂O-N L⁻¹), whereas Summer D values were very low (0.32 µg N₂O-N L⁻¹). From all campaigns, the maximum values of dissolved N₂O were measured in the shallow water column, while in the intermediate zone and the deep zones at inlet and outlet, the values were significantly lower.

Table 1. Mean values and standard errors of potential N₂ and N₂O fluxes in sediments, N₂O fluxes from open water surfaces measured with automated and manual chambers, through-flow flux of dissolved N₂O (all in $\mu\text{g N}_2\text{O-N s}^{-1}$), in Rampillon CW during the measurement campaigns. Man – manual chambers.

	N (number of measurements) per season A/W/S/SW/SD/AS	Autumn (A)	Winter (W)	Spring (S)	Summer W (SW)	Summer D (SD)	All seasons (AS)
Sediments							
N ₂ flux (potential)	40/40/20/20/40/16 0	5434 (574)	3809 (319)	4119 (979)	5085 (909)	1304 (412)	3905 (281)
N ₂ O flux (potential)	40/40/20/20/40/16 0	25 (6)	4.3 (1.3)	85 (47)	28 (53)	8 (3)	44 (20)
Water							
Dissolved N ₂ O through-flow flux	21/21/7/7/ 11/67	51.8 (17.1)	0	10.1 (3.5)	11.7 (5.8)	0	19.6 (14.4)
Atmosphere							
N ₂ O flux	1192/178/ 584/400/168/ 2522	9.2 (1.5)	2.6 (0.3)	0.9 (0.3)	0.1 (0.4)	5.4 (0.3)	3.6 (0.1)
N ₂ O flux by Man	68/70/42/44/80/30 4	11.1 (0.8)	3.8 (0.3)	1.6 (0.5)	1.8 (0.4)	-0.01 (0.3)	3.9 (0.3)
N ₂ O total average	1260/248/ 626/444/248/ 2820	9.7 (0.2)	3.2 (0.1)	0.6 (0.3)	0.2 (0.3)	4.8 (0.3)	3.7 (0.1)

The annual (mean \pm SE) amount of through-flow dissolved N₂O (water discharge multiplied by concentration) was $20\pm 14 \mu\text{g N}_2\text{O-N s}^{-1}$, being the highest in Autumn ($52\pm 17 \mu\text{g N}_2\text{O-N s}^{-1}$), moderate in Spring and Summer W, and zero in Winter (no dissolved N₂O in the water) and Summer D (no water flow; Table 1).

3.5 Potential N₂ and N₂O flux from sediments

In the lab experiments under controlled conditions, the average potential N₂ emission ($N_{2\text{potential}}$) from the sediment was very high ($3905 \mu\text{g N}_2\text{-N m}^{-2} \text{h}^{-1}$), showing relatively similar values throughout the seasons, except the Summer D period ($1304 \mu\text{g N}_2\text{-N m}^{-2} \text{h}^{-1}$; Table 1). Besides, potential N₂O flux ($N_{2\text{Opotential}}$) varied largely from -9 to $1065 \mu\text{g N}_2\text{O-N m}^{-2} \text{h}^{-1}$, showing the highest average values in Summer W and Spring and lowest ones in Winter and Summer D (Table 1). Consequently, the variation of the ratio $N_{2\text{-Npotential}} : N_{2\text{O-Npotential}}$ was also remarkable, from 48:1 in Spring to 886:1 in Winter, making up the average

annual value of 89:1 (Table 1 and Fig. S4).

3.6 Relationship of N₂O to environmental parameters

The PCA showed significant differences between groupings of sampling campaigns ($p < 0.001$; Fig. S5A) and subsites ($p < 0.01$; Fig. S5B). All seasons were significantly different from each other ($p < 0.05$), except for the low-temperature seasons (Autumn and Winter) and the high-temperature wet periods (Spring and Summer W). Although significant differences were not detected between subsites, sites from the shallow middle zone were clustered distinctly from the deeper inflow (S1 and S2) and outflow subsites (F1 and F2). The environmental parameters varied between the campaigns and sites, and the gases showed some trends (Fig. S5C). According to the PCA, the N₂O emissions were the highest in Autumn and Winter, although dissolved N₂O from water and potential N₂O emissions from the sediment showed the highest values in Spring and Summer W. Summer D had the smallest potential N₂ emissions.

The FPCA (Fig. 5) revealed that gaseous N₂O emissions from the water surface and potential N₂ flux from the topsoil were the most impacted by different physicochemical conditions showing many different and significant correlations with them. Gaseous N₂O emissions from the water surface showed strong positive correlation with water NO₃⁻ concentration, water flow and removal rate of nitrate, and strong negative correlation with water temperature, TOC_W, DOC_W and HRT. Both dissolved N₂O in water and potential N₂O flux from sediment were positively correlated to water temperature and DOC_S. Potential N₂ flux was positively correlated with water ion concentrations (Na⁺, Ca²⁺, SO₄²⁻, Cl⁻, Mg²⁺, K⁺), sediment-related parameters (pH, NH₄⁺, DOC), water flow and depth, the removal rate of nitrate, and negatively with sediment-related parameters (NO₃⁻, OM%, N%, Mg, Ca), DOC_W, and hydraulic residence time.

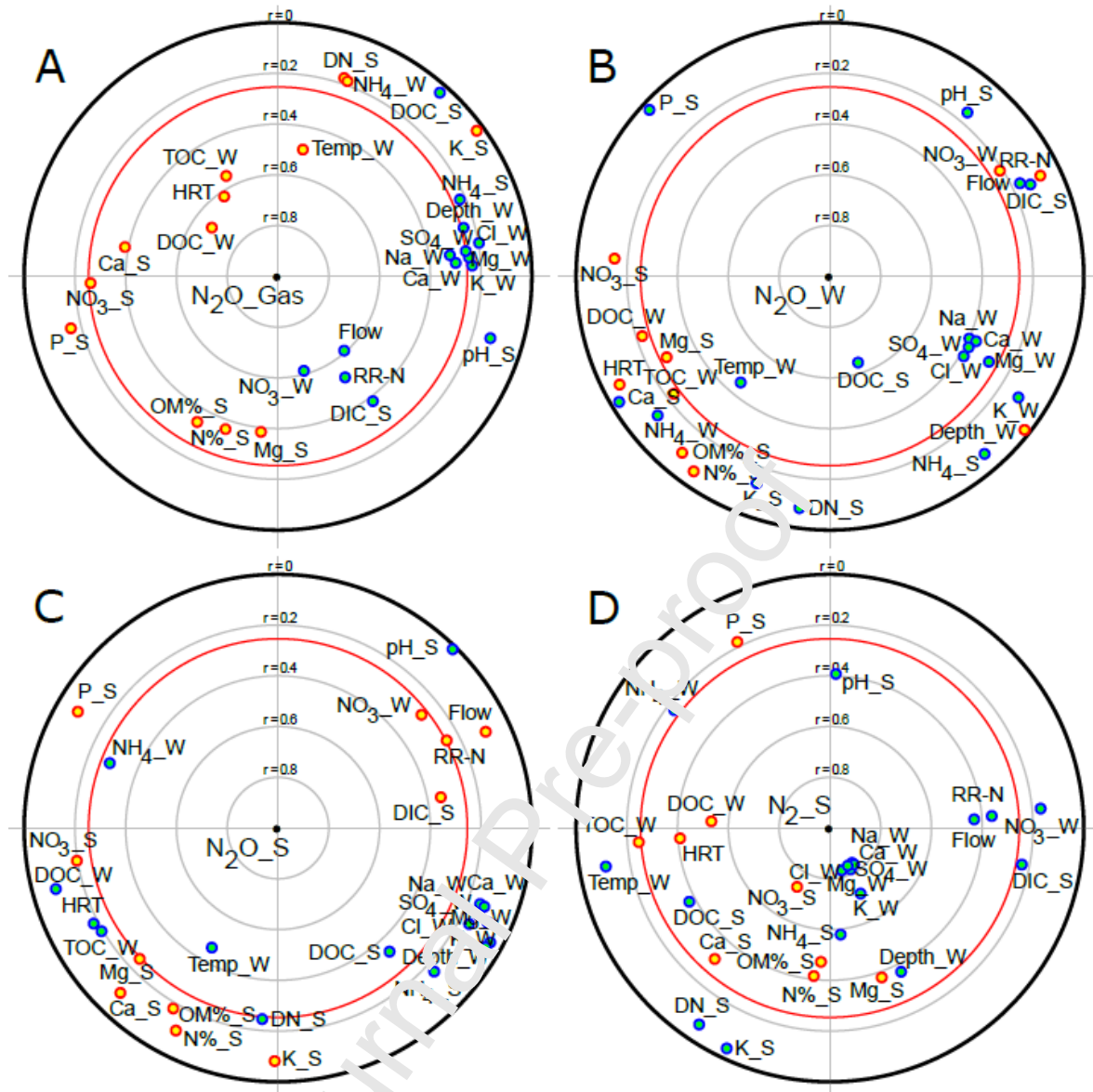


Figure 5. Focused PCA of physicochemical variables, with focus on: gaseous N_2O flux (A), dissolved in the water N_2O_W (B), and sediment N_2O_S flux (potential) (C) and N_2_S flux (potential) (D) ($n = 60$). Variables inside the red circle are significantly correlated to the dependent variable with $p < 0.05$. Turquoise filled navy blue circles are positively correlated to the dependent variable and yellow filled red circles are negatively correlated.

4 Discussion

4.1 Dynamics of gaseous N_2O emissions

The average annual emission of gaseous N_2O emissions in Rampillon was unexpectedly low: $3.7 \mu\text{g } N_2O\text{-N m}^{-2} \text{ h}^{-1}$. It represents the lowest range of emission values in the CW, which varies between -3 to $650 \mu\text{g } N_2O\text{-N m}^{-2} \text{ h}^{-1}$ (Mander et al., 2014). Our results on seasonal average N_2O emission values (0.1 to $9.2 \mu\text{g } N_2O\text{-N m}^{-2} \text{ h}^{-1}$) are lower than those measured in

an analogous CW for treating nitrate-polluted river water in Columbus, OH, USA: averaged values from 7 to 22 $\mu\text{g N}_2\text{O-N m}^{-2} \text{h}^{-1}$ by Hernandez & Mitsch (2006) and from 38 to 415 $\mu\text{g N}_2\text{O-N m}^{-2} \text{h}^{-1}$ by Batson et al. (2012). Furthermore, Glaz et al. (2017) reported low N_2O emission in waste stabilization ponds with likely complete denitrification: from 0.06 $\mu\text{g N}_2\text{O-N m}^{-2} \text{h}^{-1}$ in Western Australia to 0.84 $\mu\text{g N}_2\text{O-N m}^{-2} \text{h}^{-1}$ in Quebec, Canada.

Compared to N_2O emissions from riverine riparian zones in a similar agricultural and geological context, the values found in Rampillon CW are more than one order of magnitude lower (Billen et al., 2020).

In Rampillon, the mean value of annual emission factor (EF; $\text{N}_2\text{O-N}$ emitted / inflow NO_3^- -N) was 0.0065%, varying from 0.0025% in Winter to 0.025% in Spring. This is 20 times less than the values reported by Mander et al. (2014) for FWS CWs for wastewater treatment (based on inflow TN values) but comparable with the indirect EFs given by IPCC (2002) and Sawamoto et al. (2005): 0.015% and 0.0024%, respectively. This can be explained by nitrate as the main nitrogen form in agricultural runoff, leading to reduced nitrification or DNRA. This indicates that the source of N_2O is mainly denitrification.

Except for the Summer D period of no water flow (Fig. 2), the average N_2O emissions from automated chambers were slightly lower than those from the manual chambers (Fig. S1). This is likely due to the missing nights from the manual measurements. However, diurnal variability was smaller than the interdiurnal one (Fig. S6). Similar results have been reported from agricultural soils (Benoit et al., 2015). Averaged across the four campaigns, the manual chambers led to a minor overestimate of fluxes compared to the high-frequency measurements with the automated chambers. Also, the range of individual values measured with the automated chambers was larger than from manual ones: from -9 to 138 and from -4 to 31 $\mu\text{g N}_2\text{O-N m}^{-2} \text{h}^{-1}$, respectively. Certainly manual chambers are less adapted for capturing ebullitive fluxes, at least in the deeper water zones and during warm periods (see Fig. S6). However, during our campaigns,, most of the gaseous N_2O emissions in automated chambers were formed through the diffusion process and only 3.6% of emissions (those above 20 $\mu\text{g N}_2\text{O-N m}^{-2} \text{h}^{-1}$) were emitted by ebullition (see Fig. S7). Likewise, the minor role of ebullition in the total release of N_2O from wetlands has been shown by Gao et al. (2013). For a monitoring strategy in remote regions without power supply, manual chambers can be used with confidence.

4.2 Dynamics of dissolved N_2O

According to several experiments (Garnier et al. 2009; Audet et al., 2017; Marescaux et al., 2018), dissolved N_2O concentrations have been converted into N_2O gas emissions, whereas

higher streamflow significantly increases evasion of N_2O (Aho & Raymond, 2019). Nevertheless, this phenomenon happens at water velocity $>0.1 \text{ m s}^{-1}$, but in our CW, water velocity was that high only in the Autumn and Spring. That is why we found no significant correlation between the gaseous N_2O emissions and dissolved N_2O in the water nor between the dissolved N_2O and NO_3^- in the water. For comparison, in an agricultural river basin in Eastern China, a significant positive correlation was found between the concentrations of NO_3^- -N and dissolved N_2O -N. In our case, the characteristics did not help us evaluate N_2O emissions from concentrations in the water directly. The dissolved N_2O during the different campaigns ranged between 0 and $30 \mu\text{gN}_2\text{O-N L}^{-1}$ leading to a ratio of $\text{N}_2\text{O-N} : \text{NO}_3^-$ -N between 0 and 0.85%. Likewise, in earlier studies on riverine N_2O budgets, dissolved N_2O saturation levels exhibited a strong seasonal pattern reaching the highest, supersaturated values in the summer and the lowest equilibrium values in the winter (Beaulieu et al., 2010). Positive correlation between dissolved N_2O in the water and potential N_2O flux from the sediment (together with water temperature and DOC_{OC_2) reflects the N_2O production at the sediment interface well. However, degassing of dissolved N_2O into the atmosphere is controlled by several other factors such as redox potential of the water column (Beaulieu et al., 2011).

Based on the discharge and dissolved N_2O concentration values in the inlet, we calculated the throughflow of dissolved N_2O , which resulted in $20 \pm 14 \mu\text{g N s}^{-1}$. At the annual scale, the average throughflow of dissolved N_2O was $0.62 \text{ kg N}_2\text{O-N yr}^{-1}$. Likewise, Bruun et al. (2017) showed that dissolved N_2O flow was higher than gaseous N_2O emission. In further perspective, specific measurements of gas transfer velocity are required to enable an evaluation of gaseous N_2O emissions dissolved in stagnant waters.

The mean $\text{N}_2\text{O-N}_{\text{dissolved}} : \text{NO}_3^-$ -N ratio was 0.16%, with a peak of 0.58% in the Autumn. This shows that the proportion of dissolved N_2O -N in Rampillon CW is relatively small and the potential degassing downstream is low. Correspondingly, these values were up to 15 and 58 times lower than those found in a study conducted within riparian zones along the agriculturally impacted San Joaquin River, CA, USA (Hinshaw & Dahlgren, 2016). However, the higher throughflow of dissolved N_2O than the emission of gaseous N_2O could mean that the N_2O produced in the CW will be emitted downstream (Outram & Hiscock, 2012).

To avoid this, we advise a low $\text{N}_2\text{O-N}_{\text{dissolved}} : \text{NO}_3^-$ -N concentration ratio when designing a CW for nitrate removal.

4.3 Relationship between gaseous N_2O fluxes and environmental factors

Seasonal variations of gaseous N_2O fluxes are controlled by abiotic factors such as temperature and hydrological regime but also by DOC in the water. N_2O emission increased with higher NO_3^- water concentration and amplified with high temperature, high flow and consequently short HRT. Indeed, Autumn and Winter, albeit with similar water flows, led to strongly different N_2O emissions, due to differences in temperature, and nitrate concentrations. Dissolved N_2O also confirmed the tendency peaked in Autumn. One explanation can be different availability of DOC due to NO_3^- reduction in the water. DOC content was the lowest in Autumn, which was probably depleted in denitrification. It is well-known from previous studies that below some critical threshold of C:N ratio the N_2O emission from soils increases exponentially (Chung & Chung, 2000; Klemetsson et al., 2005). In our study, significant positive nonlinear correlation ($R^2 = 0.56$) was found between the DOC: NO_3^- -N ratio and N_2O emissions: the emission rapidly increases below a ratio of less than 5 (Fig. 6). In mid-Autumn (November), after a dry period, we can expect that most of internal DOC (formed from vegetation decay in the CW) and external DOC (possibly leached from soils in the catchment) was already consumed by denitrification and could not fuel the complete denitrification process. Therefore, denitrification stopped at the stage of N_2O emissions. In Autumn, we observed the highest N_2O emissions.

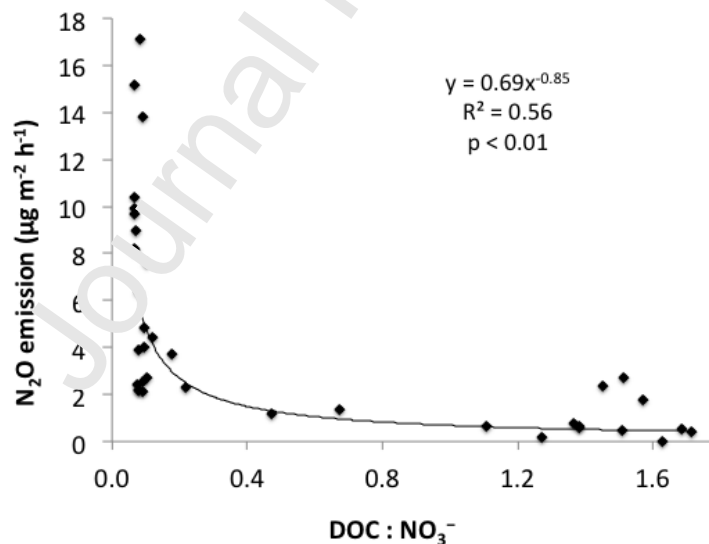


Figure 6. Relationship between N_2O emissions and DOC : NO_3^- -N as C : N ratio in the inlet of Rampillon CW.

Spring and Summer W with the highest HRT left enough time to complete the denitrification with less N_2O emissions (Table 1). It even caused consumption of N_2O (negative emission values for 52% of the time of Spring up to $-8.8 \mu g N_2O-N m^2 h^{-1}$) of N_2O , which dropped

below the saturation value in the water leading to dissolution from the atmosphere to the water column. Although this kind of consumption has been observed in several aquatic ecosystems (Beaulieu et al., 2011; Mander et al., 2014; Soued et al., 2016), it seems to be the first time that a CW is shown to turn to a sink of N_2O during warm temperature and low flow. A similar seasonal pattern to Rampillon was demonstrated in a study of Lake Neusiedl, Austria, where the highest emission rates from the water ($25\text{-}48 \mu\text{g N}_2\text{O m}^{-2} \text{h}^{-1}$) were observed in late autumn whereas N_2O was taken up mainly in the spring and occasionally in late summer and even early autumn (Soja et al., 2014).

Although nitrate concentrations in Rampillon water are high, gaseous N_2O emission is relatively low, which can be explained by a complex of environmental factors and water regime control. One of the basic determinants is the high pH and high Ca^{2+} concentration in both water and sediments (Table S1). These conditions are beneficial for the transformation of N_2O to N_2 , i.e., a complete denitrification process.

Water flow, water table and HRT are important factors influencing gaseous N_2O fluxes in Rampillon CW (Fig. 4 and Fig. S4). From previous studies, it is known that the fluctuating water table and pulsing water regime are enhancing N_2O emissions from various wetlands (Jia et al., 2011; Mander et al., 2011; Kaurhal et al., 2014). Most likely, this is due to the better aeration of temporarily inundated wetland sediments, which inhibits the full path of denitrification and enhances N_2O release from other processes such as nitrification (Ji et al., 2011), DNRA (Jahangir et al., 2017; Wang et al., 2018) and nitrifier denitrification (Masta et al., 2020). Expectedly, one could see that phenomenon in Rampillon where the water table frequently fluctuates. However, here the impact of pulsing was not so clear and appeared only at extremely low water periods when half of the bed was dry and the water stayed only in deeper parts (Summer D and also the beginning of Summer W sessions; Fig. 1, Table 1). Assumably, such short-term aeration in the dry parts could not inhibit the denitrification process (see Jørgensen & Elberling 2012) and might enhance the fast growth of vegetation. Young shoots of macrophytes and also filamentous algae mats covered the dried parts in a few days. Thus, plants might compete for N source with denitrifiers, even in such an N-saturated system (NH_4^+ content in sediment was highest during Summer D). This is supported by the fact that in Summer D, the formation of $\text{N}_{2\text{potential}}$ in the sediments was the lowest among all the campaigns ($1304 \mu\text{g N m}^{-2} \text{h}^{-1}$, i.e., 34% of the mean annual value). Likewise, $\text{N}_{2\text{Opotential}}$ was very low ($8 \mu\text{g N m}^{-2} \text{h}^{-1}$; i.e., 18%; Table 1, Fig. S4).

Several studies have analysed the influence of vascular plants in N_2O emissions from wetlands. It depends on many factors in an equilibrium between the oxygen-ruled microbial

processes (first of all denitrification vs. nitrification), plant uptake and oxygen supply to the rhizosphere, which depends on the presence of aerenchymous tissue, and age, biomass and roots development of the plants. Thus, depending on the equilibrium, wetland plants can increase (Chen et al., 2011; Jørgensen et al., 2012) or decrease (Hu et al., 2016) N_2O emissions.

As expected, the gaseous N_2O emissions were strongly linked to nitrate concentration and nitrate removal rate, DOC concentrations, and pH (Figs. 4 and 5), high pH favoring N_2O reduction (Hénault et al., 2019; Billen et al., 2020).

The annual average N_2O emission and the estimated flux of dissolved N_2O in through-flow water were 0.32 and 0.62 kg $N_2O-N\ ha^{-1}\ yr^{-1}$, respectively. Comparing the gaseous flux value to 938 kg $NO_3^- -N\ ha^{-1}\ yr^{-1}$ denitrified, we get a low $N_2O-N:NO_3^- -N$ ratio of 0.033%.

5 Conclusions

Our first hypothesis was not supported: in contrast to the expected high N_2O emissions, the Rampillon CW was a weak source of N_2O emitted to the atmosphere. The ratio of N_2O-N emitted to $NO_3^- -N$ removed was 0.034%. Likewise, losses of dissolved N_2O were relatively small in the system: the ratio of dissolved N_2O-N in the outflow to $NO_3^- -N$ removed was 0.066%. The second hypothesis was supported, our analysis showed a high denitrification potential reflected by large potential N_2 fluxes and a high $N_2:N_2O$ ratio in the sediments. All the results indicate complete denitrification in the CW. Since there was no significant diurnal pattern in the N_2O emission, the high and low frequency measurements of N_2O emission gave comparable results. We found clear seasonal variation of N_2O emissions showing the highest values in the autumn when organic carbon was mineralised, fuelling denitrifiers. This variation correlated with the temporal pattern of $NO_3^- -N$ concentrations in inlet water. In addition, streamflow and nitrate reduction rate were strongly positively correlated with the gaseous N_2O fluxes. Water temperature, TOC and DOC in the water and hydraulic retention time showed strong negative correlations with N_2O emissions.

Our study represents an off-stream CW where high denitrification potential in sediments and a complete denitrification pathway ensure satisfactory nitrate removal but very low N_2O emissions, still showing a seasonal pattern. The overall N_2O balance is not significantly affected by the flow of dissolved N_2O from the wetland. The results convince us that climate-friendly design of off-stream CWs for treating nitrate-polluted agricultural run-off should include both deep and shallow zones to maintain nitrogen removal processes in fluctuating hydrological conditions. Further studies on N_2O fluxes in analogous CWs should focus on the role of macrophytes, algae and microorganisms in the N transformation processes.

Author Agreement

ÜM, KS, JT, CC and MM (Mart Muhel) designed the study. ÜM, KS, JT, CC, ME, MM (Martin Maddison), MM (Mart Muhel), JG, JDL, EU, and KR performed the study. ÜM and JT wrote the article, KS, ME JG and JP commented on draft versions of the article. All authors have approved the final article.

Acknowledgements

The study was conducted within the framework of several scientific projects: "Efficacité des Zones Tampons" by OFB (French Office for Biodiversity, and technical group "Zones Tampons"), and HydroGES (financed by the Agency for the Environment and Mastery of Energy, ADEME). The travel was supported by two French–Estonian Parrot RTD projects "Ecological engineering for nutrient control in rural catchments" and "Process-based approach and enhanced technologies of treatment wetlands" (2014–2016). The PIREN-Seine programme and the Fédération Ile-de-France de Recherche pour l'Environnement (FIRE) are also acknowledged for their support. The authors also thank AQU'Brïe association for their support and stakeholders' involvement. This study was also supported by the Estonian Research Council (grants IUT2 16, PRG352 and MOBERC20) and by the EU through the European Regional Development Fund (Centres of Excellence ENVIRON and EcolChange, and MOBTP101 returning researcher grant by the Mobilitas Plus programme).

References

- Abe, K., Komada, M., Ookuma, A., Tanihashi, S., Banzai, K., 2014. Purification performance of a shallow free-water-surface constructed wetland receiving secondary effluent for about 5 years. *Ecol. Eng.* 69, 126–133. <http://dx.doi.org/10.1016/j.ecoleng.2014.03.040>
- Aho, K.S., Raymond, P.A., 2019. Differential response of greenhouse gas evasion to storms in forested and wetland streams. *J. Geophys. Res.- Biogeo.* 124, 649–662. <https://doi.org/10.1029/2018JG004750>
- APHA-AWWA-WEF, 2005. *Standard Methods for the Examination of Water and Wastewater*. 21th ed. American Public Health Organisation.
- Audet, J., Bastviken, D., Bundschuh, M., Buffam, I., Feckler, A., Klemedtsson, L., Laudon, H., Löfgren, S., Natchimuthu, S., Öquist, M., Peacock, M., Wallin, M., 2020. Forest streams are important sources for nitrous oxide emissions. *Glob. Change. Biol.* 26, 629–641. <https://doi.org/10.1111/gcb.14812>
- Audet, J., Wallin, M.B., Kyllmar, K., Andersson, S., Bishop, K., 2017. Nitrous oxide emissions from streams in a Swedish agricultural catchment. *Agr. Ecosys. Environ.* 236, 295–303. <https://doi.org/10.1016/j.agee.2016.12.012>
- Batson, J.A., Mander, Ü., Mitsch, W.J., 2012. Denitrification and a nitrogen budget of created riparian wetlands. *J. Environ. Qual.* 41, 2024–2032. <https://doi.org/10.2134/jeq2011.0449>
- Beaulieu, J.J., Schuster, W.D., Rebolz, J.A. 2010. Nitrous oxide emissions from a large, impounded river: The Ohio River. *Environ. Sci. Technol.* 44, 19, 7527–7533. <https://doi.org/10.1021/es1016735>
- Beaulieu, J.J., Tank, J.L., Hamilton, S.K., Wollheim, W.M., Hall Jr., R.O., Mulholland, P.J.,

- Peterson, B.J., Ashkenas, L.R., Cooper, L.W., Dahm, C.N., Dodds, W.K., Grimm, N.B., Johnson, S.L., McDowell, W.H., Poole, G.C., Valett, H.M., Arango, C.P., Bernot, M.J., Burgin, A.J., Crenshaw, C.L., Helton, A.M., Johnson, L., O'Brien, J.M., Potter, J.D., Sheibley, R.W., Sobota, D.J., Thomas, S.M., 2011. Nitrous oxide emission from denitrification in stream and river networks. *P. Natl. Acad. Sci. USA* 108 (1), 214–219. www.pnas.org/cgi/doi/10.1073/pnas.1011464108
- Benoit, M., Garnier, J., Billen, G., 2015. Temperature dependence of nitrous oxide production of a luvisolic soil in batch experiments. *Process Biochem.* 50 (1), 79-85. <http://dx.doi.org/10.1016/j.procbio.2014.10.013>
- Billen, G., Garnier, J., Gossel, A., Thieu, V., Théry, S., Hénault, C. 2020. Modeling indirect N₂O emissions along the N cascade from cropland soils to rivers. *Biogeochemistry* 148, 207-221. <https://doi.org/10.1007/s10533-020-00654-x>
- Blicher-Mathiesen, G., Hoffmann, C.C., 1999. Denitrification as a sink for dissolved nitrous oxide in a freshwater riparian fen. *J. Environ. Qual.* 28, 257-262.
- Brix, H., 1997. Do macrophytes play a role in constructed treatment wetlands? *Water Sci. Technol.* 35, 5, 11-17.
- Bruun J., Hoffmann C.C., Kjaergaard C., 2017. Convective transport of dissolved gases determines the fate of the greenhouse gases produced in reactive drainage filters. *Ecol. Eng.* 98, 1–10. <https://doi.org/10.1016/j.ecoleng.2016.10.027>
- Butterbach-Bahl, K., Baggs, E.M., Dannenmann, M., Kiese, R., Zechmeister-Boltenstern, S., 2013. Nitrous oxide emissions from soils: how well do we understand the processes and their controls? *Philos. Trans. R. Soc. Lond., B, Biol. Sci.* 368. <http://dx.doi.org/10.1098/rstb.2013.0122>
- Butterbach-Bahl, K., Willibald, G., Papen GU, 2002. Soil core method for direct simultaneous determination of N₂ and N₂O emissions from forest soils. *Plant Soil* 240 (1), 105-116.
- Chen, H., Wang, M., Wu, N., Wang, Y.F., Zhu, D., Gai, Y.H., Peng, C.H., 2011. Nitrous oxide fluxes from the littoral zone of a lake on the Qinghai-Tibetan Plateau. *Environ. Monit. Assess.* 182, 545–553. <https://doi.org/10.1007/s10661-011-1896-y>
- Chen, H.H., Williams, D., Walker, J.C., Shi, W., 2016. Probing the biological sources of soil N₂O emissions by quantum cascade laser-based ¹⁵N isotopocule analysis. *Soil Biol. Biochem.* 100, 175-181. <https://doi.org/10.1016/j.soilbio.2016.06.015>
- Cheng, F.Y., Van Meter K.J., Byrnes, D.K., Basu, N.B., 2020. Maximizing US nitrate removal through wetland protection and restoration. *Nature* 588, 625-639. <https://doi.org/10.1038/s41586-020-03042-5>
- Chmura, G.L., Kellman, L., van Ardenne, L., Guntenspergen, G.R., 2016. Greenhouse gas fluxes from salt marshes exposed to chronic nutrient enrichment. *PLoS ONE* 11 (2), e0149937. <https://doi.org/10.1371/journal.pone.0149937>
- Chung, Y.C., Chung, M.S., 2000. BNP test to evaluate the influence of C/N ratio on N₂O production in biological denitrification. *Water Sci. Technol.* 42 (3–4), 23–27.
- Collier, S.M., Ruark, M.D., Oates, L.G., Jokela, W.E., Dell, C.J., 2014. Measurement of greenhouse gas flux from agricultural soils using static chambers. *J. Vis. Exp.* 90, 52110. <https://doi.org/10.3791/52110>
- Cowan, N.J., Famulari, D., Levy, P.E., Anderson, M., Bell, M.J., Rees, R.M., Reay, D.S., Skiba, U.M., 2014. An improved method for measuring soil N₂O fluxes using a quantum cascade laser with a dynamic chamber. *Eur. J. Soil Sci.* 65 (5), 643–652. <https://doi.org/10.1111/ejss.12168>
- D'Acunha, B., Johnson, M.S., 2019. Water quality and greenhouse gas fluxes for stormwater detained in a constructed wetland. *J Environ. Manage.* 231 (1), 1232-1240. <https://doi.org/10.1016/j.jenvman.2018.10.106>
- Dowdell, R.J., Burford, J.R., Crees, R., 1979. Losses of nitrous oxide dissolved in drainage

- water from agricultural land. *Nature* 278, 342–343.
- Dray, S., Dufour, A., 2007. The ade4 package: Implementing the duality diagram for ecologists. *J. Stat. Software* 22(4), 1-20.
- Erler, D.V., Eyre, B.D., Davison, L., 2008. The contribution of anammox and denitrification to sediment N₂ production in a surface flow constructed wetland, *Environ. Sci. Technol.* 42, 9144-9150. <https://doi.org/10.1021/es801175t>
- Eugster, W., Zeyer, K., Zeeman, M., Michna, P., Zingg, A., Buchmann, N., Emmenegger, L., 2007. Methodical study of nitrous oxide eddy covariance measurements using quantum cascade laser spectrometry over a Swiss forest. *Biogeosciences* 4, 927-939. www.biogeosciences.net/4/927/2007/
- Falissard, B., 1999. Focused principal component analysis: looking at a correlation matrix with a particular interest in a given variable. *J. Comput. Graph. Stat.* 8(4), 906-912.
- Freeman, C., Lock, M.A., Hughes, S., Reynolds, B., Hudson, J.A., 1997. Nitrous oxide emissions and the use of wetlands for water quality amelioration. *Environ. Sci. Technol.* 31 (8), 2438-2440.
- Gao, Y., Liu, X.H., Yi, N., Wang, Y., Guo, J.Y., Zhang, Z.H., Yan, S.H., 2013. Estimation of N₂ and N₂O ebullition from eutrophic water using an improved bubble trap device. *Ecol. Eng.* 57, 403-412. <https://doi.org/10.1016/j.ecoleng.2013.04.020>
- Gao, Y., Zhang, Z.H., Liu, X.H., Yi, N., Zhang, L., Song, W., Wang, Y., Mazumder, A., Yan, S.H., 2016. Seasonal and diurnal dynamics of physicochemical parameters and gas production in vertical water column of a eutrophic pond. *Ecol. Eng.* 87, 313-323. <http://dx.doi.org/10.1016/j.ecoleng.2015.12.037>
- Garnier, J., Billen, G., Vilain, G., Martinez, A., Silvestre, M., Mounier, E., Toche, F., 2009. Nitrous oxide (N₂O) in the Seine river and basin: Observations and budgets. *Agric. Ecosys. Environ.* 133 (3-4), 223-233. <https://doi.org/10.1016/j.agee.2009.04.024>
- Garnier, J.A., Mounier, E.M., Laverman, A.M., Billen, G.F., 2020. Potential denitrification and nitrous oxide production in the sediments of the Seine River drainage network (France). *J. Environ. Qual.* 39, 449-459. <https://doi.org/10.2134/jeq2009.0299>
- Glaz, P., Bartosiewicz, M., Laurion, I., Reichwaldt, E.S., Maranger, R., Ghadouani, A., 2016. Greenhouse gas emissions from waste stabilisation ponds in Western Australia and Quebec (Canada). *Water Res.* 101, 64-74. <http://dx.doi.org/10.1016/j.watres.2016.05.060>
- Hansen, R., Mander, Ü., Soosar, K., Maddison, M., Lõhmus, K., Kupper, P., Kanal, A., Söber, J., 2013. Greenhouse gas fluxes in an open air humidity manipulation experiment. *Landscape Ecol.* 28(4), 637-649. <https://doi.org/10.1007/s10980-012-9775-7>
- Hargreaves, K.J., Wienhold, F.G., Klemetsson, L., Arah, J.R.M., Beverland, I.J., Fowler, D., Galle, Griffith II, B.D.W.T., Skiba, U., Smith, K.A., Welling, M., Harris, G.W. 1996. Measurement of nitrous oxide emission from agricultural land using micrometeorological methods. *Atmos. Environ.* 30 (10-11), 1563-1571.
- Haynes, W.M. (ed.) 2015. *CRC Handbook of Chemistry and Physics*. 95th Edition, 2014-2015. CRC Press LLC, Boca Raton: FL, p. 4-78.
- Hénault C., Bourennane, H., Ayzac, A., Ratié, C. Saby, N.P.A., Cohan, J.-P., Eglin, T., Le Gall, C., 2019. Management of soil pH promotes nitrous oxide reduction and thus mitigates soil emissions of this greenhouse gas. *Sci. Reports*, 9, 20182. <https://doi.org/10.1038/s41598-019-56694-3>
- Hernandez, M.E., Mitsch, W.J., 2006. Influence of hydrologic pulses, flooding frequency, and vegetation on nitrous oxide emissions from created riparian marshes. *Wetlands* 26,862–877. DOI: 10.1672/0277-5212(2006)26[862:IOHPFF]2.0.CO;2
- Hinshaw, S.E., Dahlgren, R.A., 2016. Nitrous oxide fluxes and dissolved N gases (N₂ and N₂O) within riparian zones along the agriculturally impacted San Joaquin River. *Nutr. Cycl. Agroecosys.* 105, 85–102. <https://doi.org/10.1007/s10705-016-9777-y>

- Hu, Q.W., Cai, J.Y., Yao, B., Wu, Q., Wang, Y.Q., Xu, X.L., 2016. Plant-mediated methane and nitrous oxide fluxes from a carex meadow in Poyang Lake during drawdown periods. *Plant Soil* 400 (1-2), 367-380. <https://doi.org/10.1007/s11104-015-2733-9>
- Huang, H., Wang, J., Hui, D., Miller, D.R., Bhattarai, S., Dennis, S., Smart, D., Sammis, T., Reddy, K.C., 2014. Nitrous oxide emissions from a commercial cornfield (*Zea mays*) measured using the eddy covariance technique. *Atmos. Chem. Phys.* 14 (23), 12839-12854. <https://doi.org/10.5194/acp-14-12839-2014>
- Hutchinson, G. L., Livingston, G.P., 1993. Use of Chamber Systems to Measure Trace Gas Fluxes. *Agricultural Ecosystem Effects on Trace Gases and Global Climate Change* 55, 63-78.
- IPCC. 2000. *Good Practice Guidance and Uncertainty Management in National Greenhouse Gas Inventories*. Inst. for Global Environ. Strategies, Kamiyamaguchi, Japan.
- IPCC. 2002. Indirect N₂O emissions from agriculture. In: *Background Papers, IPCC Expert Meetings on Good Practice Guidance and Uncertainty Management in National Greenhouse Gas Inventories*. Inst. for Global Environ. Strategies, Kamiyamaguchi, Japan, pp. 381–397,
- IPCC. 2007. *Climate Change 2007. The Physical Science Basis. Chapter 2: Changes in Atmospheric Constituents and in Radiative Forcing*. Cambridge University Press, Cambridge, pp. 131-234.
- IPCC. 2013. *Climate Change 2013. The Physical Science Basis. Contribution of Working Group I to the Fifth Assessment Report of the Intergovernmental Panel on Climate Change*. WMO, Geneva, 127 p.
- Jahangir, M.M.R., Fenton, O., Müller, C., Harrington, R., Johnston, P., Richards, K.G., 2017. *In situ* denitrification and DNRA rates in groundwater beneath an integrated constructed wetland. *Water Res.* 111, 254-264. <https://doi.org/10.1016/j.watres.2017.01.015>
- Jia, W., Zhang, J., Li, P., Xie, H., Wu, J., Wang, J., 2011. Nitrous oxide emissions from surface flow and subsurface flow constructed wetland microcosms: effect of feeding strategies. *Ecol. Eng.* 37 (11), 1815–1821. <https://doi.org/10.1016/j.ecoleng.2011.06.019>
- Jørgensen, C.J., Elberling, B., 2012. Effects of flooding-induced N₂O production, consumption and emission dynamics on the annual N₂O emission budget in wetland soil. *Soil Biol. Biochem.* 53, 9-17. <https://doi.org/10.1016/j.soilbio.2012.05.005>
- Jørgensen, C.J., Struwe, S., Elberling, B., 2012. Temporal trends in N₂O flux dynamics in a Danish wetland – effects of plant-mediated gas transport of N₂O and O₂ following changes in the water level and soil mineral-N availability. *Glob. Change Biol.* 18 (1), 210-222. <https://doi.org/10.1111/j.1365-2486.2011.02485.x>
- Jurado, A., Borges, V., Bouyère, S. 2017. Dynamics and emissions of N₂O in groundwater: A review. *Sci. Total Environ.* 584–585, 207–218. <http://dx.doi.org/10.1016/j.scitotenv.2017.01.127>
- Kasper, M., Foldal, C., Kitzler, B., Haas, E., Strauss, P., Eder, A., Zechmeister-Boltenstern, S., Amon, B., 2019. N₂O emissions and NO₃⁻ leaching from two contrasting regions in Austria and influence of soil, crops and climate: a modelling approach. *Nutr. Cycl. Agroecosyst.* 113, 95–111. <https://doi.org/10.1007/s10705-018-9965-z>
- Kaushal, S.S., Mayer, P.M., Vidon, P.G., Smith, R.M., Pennino, M.J., Tamara A. Newcomer, T.A., Duan, S.W., Welty, C., Belt, K.T., 2014. Land use and climate variability amplify carbon, nutrient, and contaminant pulses: A review with management implications. *J. Am. Water Resour. As. (JAWRA)* 50 (3), 585-614.
- Klemetsson, L., Von Arnold, K., Weslien P., Gundersen, P., 2005. Soil CN ratio as a scalar parameter to predict nitrous oxide emissions. *Glob. Change Biol.* 11 (7), 1142-1147. <https://doi.org/10.1111/j.1365-2486.2005.00973.x>
- Li, J.H., Yang, X.Y., Wang, Z.F., Shan, Y., Zheng, Z., 2015. Comparison of four aquatic

- plant treatment systems for nutrient removal from eutrophied water. *Bioresource Technol.* 179, 1-7. <http://dx.doi.org/10.1016/j.biortech.2014.11.053>
- Ligi, T., Truu, M., Oopkaup, K., Nõlvak, H., Mander, Ü., Mitsch, W.J., Truu, J., 2015. Genetic potential of N₂ emission via denitrification and ANAMMOX from the soils and sediments of a created riverine treatment wetland complex. *Ecol. Eng.* 80, 181-190. <http://dx.doi.org/10.1016/j.ecoleng.2014.09.072>
- Lindau, C.W., DeLaune, R.D., 1991. Dinitrogen and nitrous oxide emission and entrapment in *Spartina alterniflora* salt marsh soils following addition of N-15 labeled ammonium and nitrate. *Estuar. Coast. Shelf S.* 32, 2, 161-172. [https://doi.org/10.1016/0272-7714\(91\)90012-Z](https://doi.org/10.1016/0272-7714(91)90012-Z)
- Lindau, C.W., DeLaune, R.D., Jiraporncharoen, S., Manajuti, D., 1991. Nitrous oxide and dinitrogen emissions from *Panicum hemitomon* S. freshwater marsh soils following addition of N-15 labeled ammonium and nitrate. *J. Freshwater Ecol.* 6, 2, 191-198. <https://doi.org/10.1080/02705060.1991.9665293>
- Livingston, G.P., Hutchinson, G.L., 1995. Enclosure-based measurement of trace gas exchange: Applications and sources of error. In: Matson, P.A., Harris, R.C., (eds.) *Biogenic Trace Gases: Measuring Emissions from Soil and Water*. Ed. Blackwell Publishing: Oxford, United Kingdom, pp. 14–51.
- Ma, L., Liu, W., Tan, Q.Y., Zhou, Q.H., Wu, Z.B., He, F., 2016. Quantitative response of nitrogen dynamic processes to functional gene abundances in a pond-ditch circulation system for rural wastewater treatment. *Ecol. Eng.* 134, 101-111. <http://dx.doi.org/10.1016/j.ecoleng.2016.05.031>
- Maavara, T., Lauerwald, R., Laruelle, G.G., Akbarzadeh, Z., Bouskill, N.J., Van Cappellen P., Regnier, P., 2019. Nitrous oxide emissions from inland waters: Are IPCC estimates too high? *Glob. Change Biol.* 2, 473-489. <https://doi.org/10.1111/gcb.14504>
- Mayer, M. 2019. Package ‘missRanger’. R Package.
- Mander, Ü., Dotro, G., Ebbe, Y., Fowprayoon, S., Chiemchaisri, C., Nogueira, S.F., Jamsranjav, B., Kasak, K., Truu, J., Tournebise, J., Mitsch, W.J., 2014. Greenhouse gas emission in constructed wetlands for wastewater treatment: a review. *Ecol. Eng.* 66, 19-35. <http://dx.doi.org/10.1016/j.ecoleng.2013.12.006>
- Mander, Ü., Maddison, M., Sosaar, K., Karabelnik, K., 2011. The impact of intermittent hydrology and fluctuating water table on greenhouse gas emissions from subsurface flow constructed wetlands for wastewater treatment. *Wetlands* 31 (6), 1023-1032. <https://doi.org/10.1007/s1157-011-0218-z>
- Mander, Ü., Teiter, S., Augustin, J., 2005. Emission of greenhouse gases from constructed wetlands for wastewater treatment and from riparian buffer zones. *Water Sci. Technol.* 52 (11-12), 167-176.
- Marescaux, A., Thieu, V., Garnier, J., 2018. Carbon dioxide, methane and nitrous oxide emissions from the human-impacted Seine watershed in France. *Sci. Total Environ.* 643, 247-259. <https://doi.org/10.1016/j.scitotenv.2018.06.151>
- Masta, M., Sepp, H., Pärn, J., Kirsimäe, K., Mander, Ü., 2020. Natural nitrogen isotope ratios as a potential indicator of N₂O production pathways in a floodplain fen. *Water* 12 (2), 409. <https://doi.org/10.3390/w12020409>
- Merböld, L., Eugster, W., Stieger, J., Zahniser, M., Nelson, D., Buchmann, N., 2014. Greenhouse gas budget (CO₂, CH₄ and N₂O) of intensively managed grassland following restoration. *Glob. Change Biol.* 20 (6), 1913-1928. <https://doi.org/10.1111/gcb.12518>
- Nelson, D.D., MaManus, B., Urbanski, S., Herndon, S., Zahniser, M., 2004. High precision measurements of atmospheric nitrous oxide and methane using thermoelectrically cooled mid-infrared quantum cascade lasers and detectors. *Spectrochim. Acta A* 60, 3325-3335. <https://doi.org/10.1016/j.saa.2004.01.033>

- Oksanen, J., Blanchet, F.G., Friendly, M., Kindt, R., Legendre, P., McGlinn, D., Minchin, P.R., O'Hara, R.G., Simpson, G.L., Solymos, P., Stevens, M.H.H., Szoecs E., Wagner, H. 2019. *vegan*: Community Ecology Package. R package version 2.5-6. <http://CRAN.Rproject.org/package=vegan>
- Outram, F.N., Hiscock, K.M., 2012. Indirect nitrous oxide emissions from surface water bodies in a lowland arable catchment: A significant contribution to agricultural greenhouse gas budgets? *Environ. Sci. Technol.* 46, (15), 8156-8163. <http://dx.doi.org/10.1021/es3012244>
- Paludan, C., Blicher-Mathiesen, G., 1996. Losses of inorganic carbon and nitrous oxide from a temperate freshwater wetland in relation to nitrate loading. *Biogeochemistry* 35, 305-326.
- Pulou, J., Tournebize, J., Chaumont, C., Haury, J., Laverman, A.M., 2012. Carbon availability limits potential denitrification in the watercress farm sediment. *Ecol. Eng.* 49, 212-220. <http://dx.doi.org/10.1016/j.ecoleng.2012.08.002>
- Ravishankara, A.R., Daniel, J.S., Portmann, R.W., 2009. Nitrous oxide (N₂O): The dominant ozone-depleting substance emitted in the 21st century. *Science* 326 (5949), 123-125. <https://doi.org/10.1126/science.1176985>
- Roper, J.D., Burton, D.L., Madani, A., Stratton, C.W., 2013. A simple method for quantifying dissolved nitrous oxide in tile drainage water. *Can. J. Soil Sci.* 93, 59-64. <https://doi.org/10.4141/CJSS2012-021>
- Savage, K., Phillips, R., Davidson, E., 2014. High temporal frequency measurements of greenhouse gas emissions from soils. *Biogeosciences* 11 (10), 2709-2720. <https://doi.org/10.5194/bg-11-2709-2014>
- Sawamoto, T., Nakajima, Y., Kasuya, M., Tsuruta, H., Yagi, K., 2005. Evaluation of emission factors for indirect N₂O emission due to nitrogen leaching in agro-ecosystems. *Geophys. Res. Lett.* 32, L03403. <https://doi.org/10.1029/2004GL021625>
- Soja, G., Kitzler, B., Soja, A.-M. 2014., Emissions of greenhouse gases from Lake Neusiedl, a shallow steppe lake in Eastern Austria. *Hydrobiologia* 731, 125–138. <https://doi.org/10.1007/s10750-013-1681-8>
- Sosaar, K., Mander, Ü., Maddison, M., Kanal, A., Kull, A., Lõhmus, K., Truu, J., Augustin, J., 2011. Dynamics of gaseous nitrogen and carbon fluxes in riparian alder forests. *Ecol. Eng.* 37 (1), 40-53. <https://doi.org/10.1016/j.ecoleng.2010.07.025>
- Soued, C., del Giorgio, P.A., Maranger, R., 2016. Nitrous oxide sinks and emissions in boreal aquatic networks in Quebec. *Nat. Geosci.* 9 (2), 116-120. <https://doi.org/10.1038/NGEO2611>
- Tournebize, J., Chaumont, C., Mander, Ü., 2017. Implications for constructed wetlands to mitigate nitrate and pesticide pollution in agricultural drained watersheds. *Ecol. Eng.* 103, 415-425. <http://dx.doi.org/10.1016/j.ecoleng.2016.02.014>
- Verhoeven, J.T.A., Arheimer, B., Yin, C.Q., Hefting, M.M., 2006. Regional and global concerns over wetlands and water quality. *Trends Ecol. Evol.* 21 (2), 96-103. <https://doi.org/10.1016/j.tree.2005.11.015>
- Vilain, G., Garnier, J., Tallec, G., Tournebize J. 2012. Indirect N₂O emissions from shallow groundwater in an agricultural catchment (Seine Basin, France). *Biogeochemistry* 111, 253–271. <https://doi.org/10.1007/s10533-011-9642-7>
- Wang, H.X., Zhang, L., Yao, X.L., Xue, B., Yan, W.J., 2017. Dissolved nitrous oxide and emission relating to denitrification across the Poyang Lake aquatic continuum. *J Environ. Sci.* 52, 130-140. <http://dx.doi.org/10.1016/j.jes.2016.03.021>
- Wang, S.Y., Wang, W.D., Liu, L., Zhuang, L.J., Zhao, S.Y., Su, Y., Li, Y.X., Wang, M.Z., Wang, C., Xu, L.Y., Zhu, G.B., 2018. Microbial nitrogen cycle hotspots in the plant-bed/ditch system of a constructed wetland with N₂O mitigation. *Environ. Sci. Technol.* 52

- (11), 6226-6236. <https://doi.org/10.1021/acs.est.7b04925>
- Wilcock, R.J., Sorrell, B.K., 2008. Emissions of greenhouse gases CH₄ and N₂O from low-gradient streams in agriculturally developed catchments. *Water Air Soil Pollut.* 188, 155–170. <https://doi.org/10.1007/s11270-007-9532-8>
- Xiao, Q.T., Hu, Z.H., Fu, C.S., Bian, H., Lee, X.H., Chen, S.T., Dongyao Shang, D.Y., 2019. Surface nitrous oxide concentrations and fluxes from water bodies of the agricultural watershed in Eastern China. *Environ. Pollut.* 251, 185-192. <https://doi.org/10.1016/j.envpol.2019.04.076>
- Yao, Z.S., Zheng, X.H., Xie, B.H., Liu, C.Y., Mei, B.L., Dong, H.B., Butterbach-Bahl, K., Zhu, J.G., 2009. Comparison of manual and automated chambers for field measurements of N₂O, CH₄, CO₂ fluxes from cultivated land. *Atmos. Environ.* 43, 11, 1888-1896. <https://doi.org/10.1016/j.atmosenv.2008.12.031>
- Zhang, X.W., Hu, Z., Zhang, J., Fan, J.L., Ngo, H.H., Guo, W.S., Zeng, C.J., Wu, Y.W., Wang, S.Y., 2018. A novel aerated surface flow constructed wetland using exhaust gas from biological wastewater treatment: Performance and mechanisms. *Biores. Technol.* 250, 94-101. <https://doi.org/10.1016/j.biortech.2017.08.179>

Declaration of competing interests

X The authors declare that they have no known competing financial interests or personal relationships that could have appeared to influence the work reported in this paper.

The authors declare the following financial interests/personal relationships which may be considered as potential competing interests:

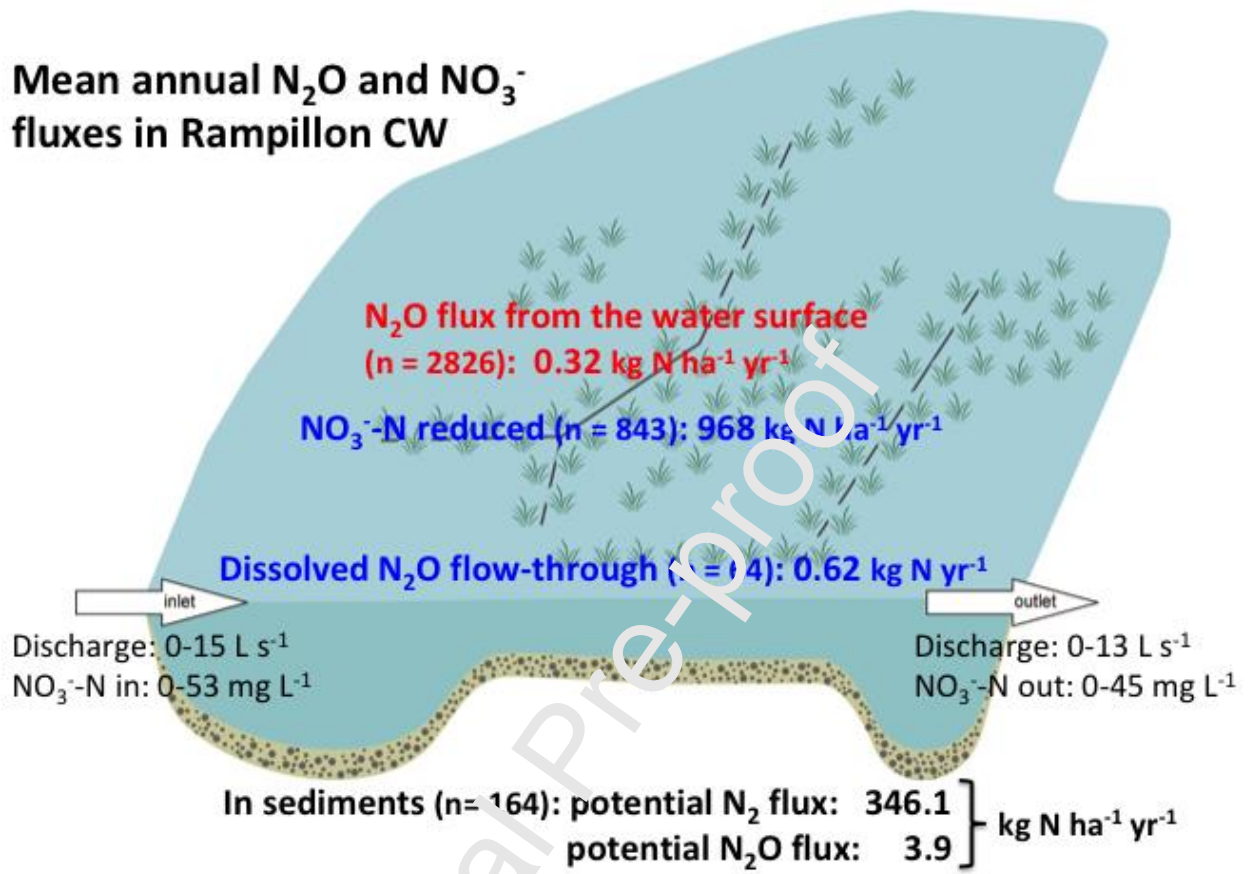
Journal Pre-proof

CRedit author statement

Ülo Mander: Conceptualization, Methodology, Investigation (field studies), Validation, Writing, Reviewing, Editing, Supervision; **Julien Tournebize:** Conceptualization, Methodology, Investigation (field studies), Validation, Writing, Editing, Supervision; **Mikk Espenberg:** Software, Data curation, Validation, Visualization, Writing; **Cedric Chaumont:** Methodology, Investigation, Validation; **Raili Torga:** Investigation (field studies), Data curation; **Josette Garnier:** Methodology, Investigation (laboratory analyses), Data curation, Validation, Writing; **Mart Muhel:** Methodology, Investigation (field studies); **Martin Maddison:** Methodology, Investigation (laboratory analyses), **Jérémie D. Lebrun:** Software, Data curation, Writing; **Emmanuelle Uher:** Software, Data curation; **Kalle Remm:** Software, Data curation; **Jaan Pärn:** Writing, Reviewing, Editing; **Kaido Soosaar:** Methodology, Investigation (field studies), Validation, Writing, Reviewing.

Graphical Abstract

Mean annual N_2O and NO_3^- fluxes in Rampillon CW



Highlights

- Low N₂O fluxes were found in an off-stream wetland treating NO₃⁻ polluted run-off
- A high potential of N₂ formation is supported by high N₂-N : N₂O-N ratio in sediments
- From the potential N₂O emission in sediments, only 9% was emitted to the atmosphere
- Analogous wetlands can be efficient in nitrate removal from agricultural runoff

Journal Pre-proof